

RESEARCH PAPER



## A novel human lncRNA SNT1 *cis*-regulates the expression of SLC47A2 by altering SFPQ/E2F1/HDAC1 binding to the promoter region in renal cell carcinoma

Zhangzhao Gao<sup>a\*</sup>, Mengjiao Chen<sup>a\*</sup>, Xueke Tian<sup>a</sup>, Lu Chen<sup>a</sup>, Le Chen<sup>a</sup>, Xiaoli Zheng<sup>a</sup>, Hua Wang<sup>b</sup>, Jinchao Chen<sup>b</sup>, An Zhao<sup>b</sup>, Qingqing Yao<sup>a</sup>, Qianying Zhu<sup>a</sup>, Shengnan Jin<sup>a</sup>, Haihong Hu<sup>a</sup>, Su Zeng<sup>a</sup>, and Lushan Yu<sup>a</sup>

<sup>a</sup>Institute of Drug Metabolism and Pharmaceutical Analysis, Zhejiang Province Key Laboratory of Anti-Cancer Drug Research, College of Pharmaceutical Sciences, Zhejiang University, Hangzhou, China; <sup>b</sup>Zhejiang Cancer Hospital, Hangzhou, China

### ABSTRACT

*SLC47A2* encodes MATE 2-K in the kidney, which mediates the secretion of certain endogenous and exogenous compounds. *SLC47A2* was dramatically repressed in patients with renal cell carcinoma (RCC), and a lower level of *SLC47A2* might act as a negative prognostic marker, although the mechanism is not well understood. In this study, we aimed to investigate the mechanism *via* which *SLC47A2* is down-regulated in RCC. Based on the annotation information of the *SLC47A2* locus available in the UCSC genome browser database, we identified a novel lncRNA, which is transcribed from the *SLC47A2* locus and named it SNT1. Overexpression and knock-down assays were performed to investigate the effects of SNT1 on *cis*-regulation of *SLC47A2*. We verified the direct binding between SNT1 and SFPQ/E2F1/HDAC1 using the cross-linking and immunoprecipitation (CLIP) assay. Chromatin immunoprecipitation was performed to confirm the molecular mechanism *via* which SNT1 activates the transcription of the *SLC47A2* coding region. We observed that SNT1 can *cis*-regulate its own genetic locus. In tumour-adjacent tissues, the *SLC47A2* locus highly expresses SNT1, which can remove the regulatory SFPQ/E2F1/HDAC1 suppressor complex from the promoter region, thereby significantly increasing the levels of the H3K27ac modification and RNAPII binding. Owing to a low SNT1 level, the binding of this inhibitory complex in the promoter region is upregulated in RCC, which results in silencing of the *SLC47A2* coding region. In conclusion, we identified a novel lncRNA and elucidated the mechanism *via* which it regulates *SLC47A2* expression in RCC.

### ARTICLE HISTORY

Received 22 November 2018  
Revised 13 February 2019  
Accepted 26 March 2019

### KEYWORDS

SNT1; SLC47A2; lncRNA; renal cell carcinoma; epigenetics

### Introduction





Renal cell carcinoma (RCC) represents 2–3% cases among all cancers, and is the most common form of kidney cancer [1]. More than 300,000 new patients are diagnosed with RCC worldwide every year [2]. Therefore, understanding the molecular biology of RCC formation and progression is critical for facilitating early diagnosis and developing new therapeutics.

Reports show that RCC is associated with epigenetic modifications of drug transporters. The human organic cation transporter 2 (*OCT2/SLC22A2*) is downregulated in the proximal tubules of RCC tumour tissues in humans because of methylation of CpG islands around the transcription start sites (TSS) of *SLC22A2* [3,4]. In addition, MATE 2-K/*SLC47A2* is also strongly repressed in RCC [5]. MATE 2-K, encoded by *SLC47A2*, is highly expressed in human kidney and mediates the secretion of both endogenous and exogenous compounds. Carnitine and creatinine are the endogenous substrates, and cimetidine, procaine, cisplatin, and oxaliplatin are exogenous substrates of MATE 2-K [6–8]. The balance between H3K4me3 and H3K27me3, and HDAC10 action are responsible for *SLC47A2* repression in RCC. H3K4me3 and H3K27me3 provide bivalent regulation of *SLC47A2* expression, whereas HDAC10 prevents


H3K27ac enrichment at the *SLC47A2* promoter, which forms a link between histone deacetylation and methylation [5].

In addition to DNA methylation and histone modifications, non-coding RNAs (ncRNAs) constitute another epigenetic mechanism *via* which gene expression is regulated. ncRNAs comprise several groups such as miRNA, siRNA, cirRNA, and lncRNA. lncRNAs are more than 200 nucleotide-long endogenous ncRNAs that can regulate gene expression, and are closely correlated with the occurrence and development of diseases [9–11]. lncRNAs perform various regulatory roles, for example, they act as transcriptional regulators, microRNA sponges, scaffolds for protein complexes, and molecular baits in gene regulation [12]. A growing body of evidence indicates that lncRNAs can regulate gene expression at the transcriptional level. For instance, the lncRNA ANCR promotes the enrichment of EZH2 at the *Runx2* promoter region and inhibits gene expression by reducing H3K27me3 modification [13].

In preliminary studies, we have observed that MATE 2-K is silenced in RCC, and histone H3K27ac, H3K4me3, and H3K27me3 modifications are involved in regulating gene expression [5]. However, the role of other epigenetic mechanisms

**CONTACT** Su Zeng  [zengsu@zju.edu.cn](mailto:zengsu@zju.edu.cn)  Zhejiang Province Key Laboratory of Anti-Cancer Drug Research; Lushan Yu  [yuls@zju.edu.cn](mailto:yuls@zju.edu.cn)  Institute of Drug Metabolism and Pharmaceutical Analysis, College of Pharmaceutical Sciences, Zhejiang University, Hangzhou 310006, China

\*These authors contributed equally to this work.

 Supplemental data for this article can be accessed [here](#).

© 2019 Informa UK Limited, trading as Taylor & Francis Group

involving ncRNAs in the regulation of *SLC47A2* expression is still unclear. In this study, we identified a novel lncRNA, SANTI1, which can *cis*-regulate MATE 2-K expression, and identified the regulatory factors involved in forming the RNA-protein (RNP) complex. We further assessed the binding of the regulatory complex at the *SLC47A2* promoter by altering SANTI1 expression, and finally demonstrated the molecular mechanism *via* which SANTI1 *cis*-regulates *SLC47A2* expression.

## Results

### Expression pattern of *SLC47A2* mRNA and SANTI1 in kidney cancer

To determine the changes in the expression of *SLC47A2* in RCC and paired adjacent normal tissues, its mRNA and protein levels were detected using reverse transcription-quantitative polymerase chain reaction (RT-qPCR) and western blotting, respectively. *SLC47A2* mRNA and protein levels were dramatically lower in RCC tissues than in adjacent normal tissues (Figure 1(a,b)).

To determine the correlation between *SLC47A2* and prognosis, the univariate test was performed using the Kaplan Meier (KM) plotter database. For renal clear cell carcinoma and renal papillary cell carcinoma, low *SLC47A2* expression was shown to be associated with poor prognosis ( $p = 0.0046$  and  $p = 0.0046$ , respectively) (Figure 1(c)).

The molecular mechanism *via* which *SLC47A2* is suppressed in RCC is still not well understood. In this study, we investigated whether ncRNAs regulated *SLC47A2* suppression. The gene could be regulated by RNAPII occupancy, transcription factor binding, and histone modifications. According to the annotation information from the UCSC genome browser, the *SLC47A2* locus might contain four potential promoters (P1-P4) and three transcription factor-binding regions (section 1–3) (Figure S1). The P1 is next to an upstream TSS; P2 is a promoter from both EPD and GeneHancer database; P3 and P4 exhibit abundant RNAPII and Ribosome binding, and they are transcription factor-binding regions too. Three transcription factor-binding regions could be found in ORegAnno section. As shown in Figure 1(d), section 1, which is located upstream of the coding mRNA's TSS, regulates the expression of its coding gene. However, sections 2 and 3 located in the intronic regions of the *SLC47A2* locus might be involved in expressing the SANTS, which might *cis*-regulate the expression of its coding gene and is also closely related to the especially lower expression level of MATE 2-K in RCC.

To determine the function of sections 2 and 3 in regulating the expression of SANTS in RCC, we determined the S-5-P RNAPII binding levels in these transcription factor-binding regions from tumour (R39C) and adjacent (R39N) tissues. We observed that sections 1 (P1 and P2) and 3 displayed significantly lower binding of S-5-P RNAPII in tumour tissue, which suggested lower transcription levels of downstream regions (Figure 1(e)). According to the location of sections 1–3 in the *SLC47A2* locus, lower S-5-P RNAPII binding in section 1 corresponded with the lower expression level of MATE 2-K in RCC; section 3, but not section 2, was essential for differential expression of SANTI in RCC. To

further confirm the relationship between SANTI and two non-mRNA-associated transcription factor-binding regions, we determined the expression levels of non-mRNA sequences located downstream of the regulatory regions using qPCR (Figure 1(f)). The transcript abundance of non-mRNA sequences from another two paired tissues were provided in Figure S2. We observed that although both sites A–D (regulated by section 2) and E (regulated by section 3) showed significantly higher expression level in adjacent tissue than in the paired tumour tissue, and the abundance of transcripts from site E was higher than those from other sites. This indicated that section 3 is the most important non-mRNA-associated transcription factor-binding region regulating the expression of SANTI in RCC. SANTI controlled by section 3 was named SANTI1.

SANTI1 expression from site E of eight RCC tissues (RC) and paired adjacent tissues (RN) was detected using qPCR. Similar to the *SLC47A2* mRNA level, SANTI1 was downregulated in RCC (Figure 1(g)). To confirm the sequence of SANTI1, the strand-specific qPCRs were carried out. As a result, SANTI1 could only be amplified in the sample that reverse transcribed by the Anti-sense primer of site E, and no coding gene transcript could be detected in the samples that reverse transcribed by the Sense or Anti-sense primer of site E (Figure S2). Furthermore, the section 3 is located in the upstream of site E, it seemed that the transcription direction of SANTI1 is same to *SLC47A2* mRNA. Considering the expression pattern of SANTI1, it might regulate *SLC47A2* *via cis* transcriptional regulation and is closely related to lower expression of MATE 2-K in RCC.

### SANTI1 up-regulated the expression of the *SLC47A2* coding region

To investigate the role of SANTI1 in regulating the expression of *SLC47A2*, we obtained the full-length sequence of SANTI1 using 5'/3' rapid amplification of cDNA ends (RACE) (Figure S3) and cloned it in an expression vector. The whole sequence of SANTI1 is transcribed from the intron *SLC47A2* locus and the SANTI1 is one member of intronic lncRNA, which is a common form of lncRNA categories (Figure S3).

The SANTI1 plasmid was transfected into 786-O, ACHN, 769-P, and Caki-1 cell lines, and the total RNA and protein were harvested 48 h after transfection. Interestingly, SANTI1 significantly upregulated the expression of *SLC47A2* in all four cell lines, irrespective of cellular heterogeneities (Figure 2(a,c)). The total RNA was also harvested at 72 h after transfection, and similar results were found (Figure S4). The expression of other drug transporters were also determined, which showed that the expression of *SLC47A1*, *ABCB1*, *ABCC2*, and *ABCC4* did not change in the presence of high levels of SANTI1 (Figure S5), demonstrating the regulatory function of SANTI1 in upregulating its own genetic locus. We further constructed a *SLC47A2* coding mRNA expression vector and observed that the expression levels of SANTI1 in four RCC cells were not induced by high levels of the mRNA (Figure 2(b)). This confirmed that SANTI1 is definitely an upstream regulator in the SANTI1-mRNA regulatory network. Several targeted siRNAs (Figure S6) were designed to knock-down the expression of the *SLC47A2* mRNA (simRNAs) and

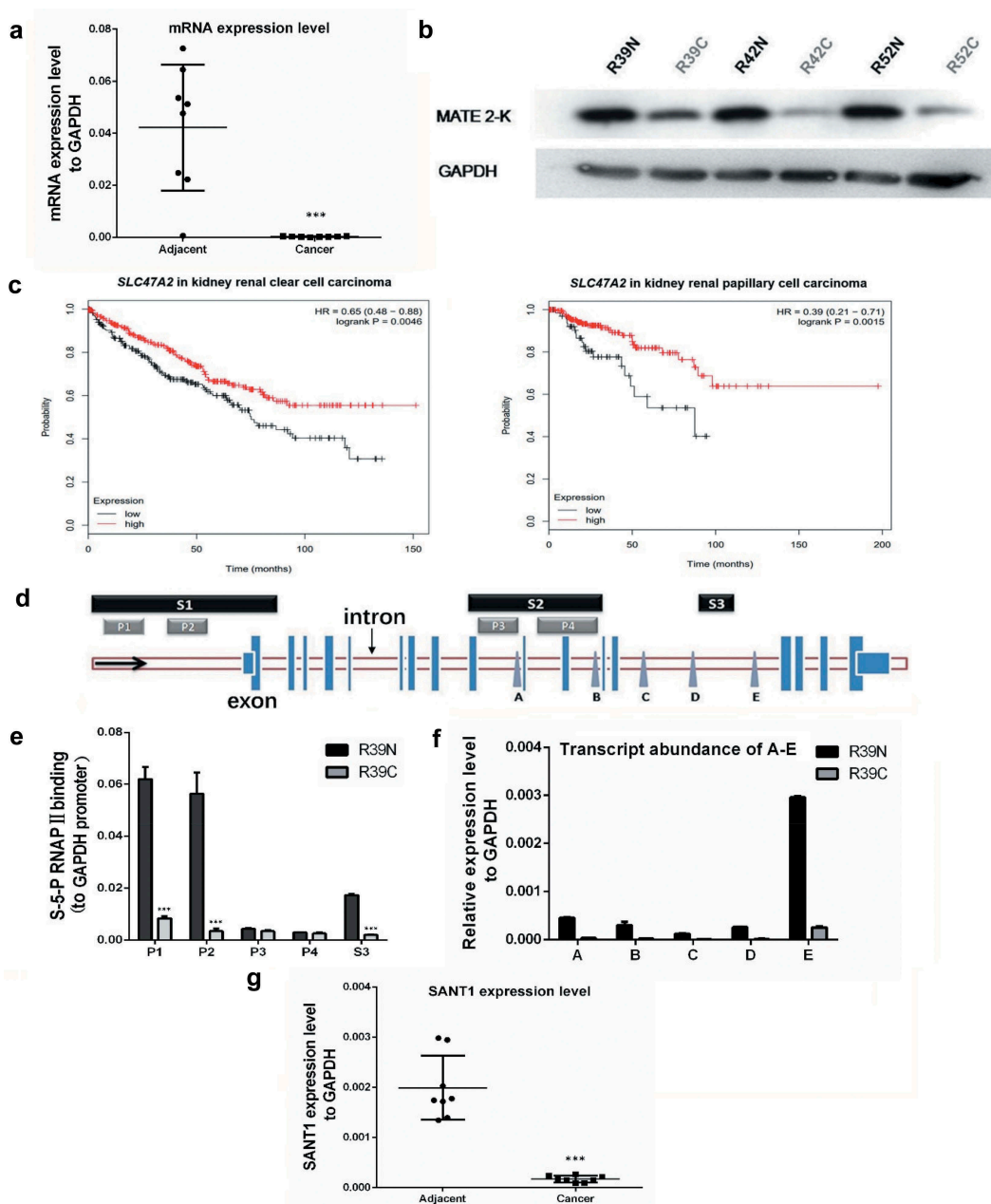


**Figure 1.** The expression levels of *SLC47A2* and *SANT1* in RCC tissues were significantly lower than in paired adjacent tissues. (a) The abundance of the *SLC47A2* mRNA was strongly reduced in tumour tissues and the expression levels were normalized to GAPDH level ( $n = 8$ ). (b) The protein levels of MATE 2-K in three RCC tissues (RC) and paired adjacent non-tumour (RN) tissues; the expression levels were normalized to GAPDH level. (c) Kaplan–Meier curves were used to determine the survival probability. Low *SLC47A2* expression indicated poor prognosis in kidney renal clear cell carcinoma ( $p = 0.0046$ ) and kidney renal papillary cell carcinoma ( $p = 0.0046$ ). (d) The UCSC genome browser revealed the locations of the promoters (P1–P4) and transcription factor (TF) binding sites (S1–S3) in the *SLC47A2* locus. The expression levels of non-mRNA transcripts (site A–E) were detected using qPCR. (e) Higher binding levels of S-5-P RNAPII on sections 1 and 3 indicated higher expression levels of mRNA and *SANT1* in adjacent tissue (R39N) than in RCC tissue (R39C). All the data were normalized to the RNAP II binding values in GAPDH promoter. (f) Transcript abundance in the downstream regulatory regions of the *SLC47A2* locus. (g) The transcript abundances of *SANT1* was strongly reduced in tumor tissues and the expression levels were normalized to that of GAPDH ( $n = 8$ ).

*SANT1* (si*SANT1*s). The siRNAs were transfected into RCC cells and the expression levels of *SLC47A2* were determined using qPCR (Figure 2(d)) and western blot analysis (Figure 2(e)). We observed that *SANT1* inhibition significantly reduced the expression of the coding region, which further demonstrated the role of *SANT1* in MATE 2-K regulation.

We harvested 769-P cells, which highly expressing *SANT1* or *SLC47A2* mRNA, and evaluated the S-5-P RNA polymerase II (RNAPII) binding rate in section 1, which indicated the

transcriptional activity of the coding region. As shown in Figure 2(f), overexpression of the *SLC47A2* coding mRNA showed similar S-5-P RNAPII binding level in the negative control, indicating that the coding mRNA was not involved in transcriptional activation in 769-P cells. However, *SANT1* strongly promoted activation of the coding gene promoter.

In conclusion, we confirmed that *SANT1* enhanced the expression of the coding region by enhancing the activity of the *SLC47A2* promoter.

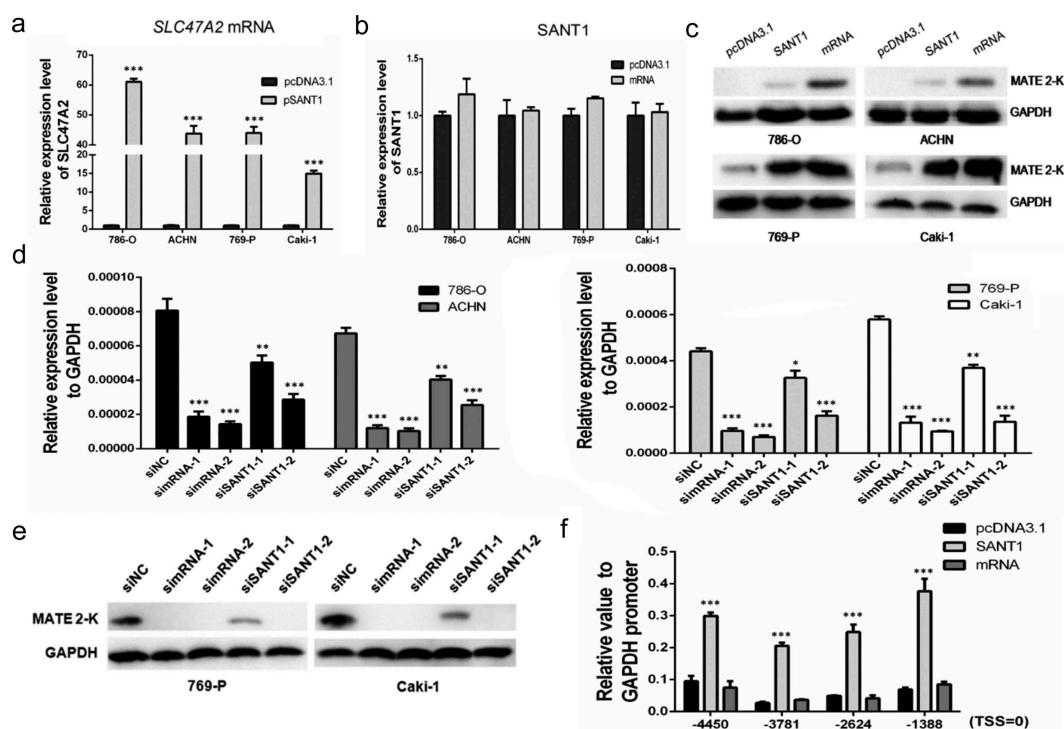


**Figure 2.** SANTI overexpression enhanced *SLC47A2* expression in RCC cell lines. (a,c) SANTI upregulated the expression of *SLC47A2* mRNA and MATE 2-K. (b) SANTI expression levels in *SLC47A2* mRNA overexpressing cells. (d, e) Four RCC cell lines were transfected with the *SLC47A2* mRNA or SANTI siRNA. *SLC47A2* expression was significantly reduced. (f) The coding gene promoter was strongly upregulated by SANTI in 769-P cells.

### The SANTI secondary structure is essential for promoting transcription of the *SLC47A2* coding region

Previous studies have reported that ncRNAs participate in gene transcriptional regulation by forming numerous RNP complexes [14] or coding micropeptides [15,16]. To further understand the mechanism *via* which SANTI regulates gene expression, we analysed the secondary structure of SANTI and then constructed two types of SANTI mutants (named SANTI-S1 and SANTI-S2). We amplified a certain sequence from the 3' terminus of SANTI and sub-cloned the amplified products into pcDNA3.1 (+) with two different enzyme digestion schemes (Figure S2). As a result, these two SANTI mutants exhibited identical fundamental sequence and translation potency but dramatically different secondary structures (Figure 3(a)). To confirm the transcriptional start site of the rescued transcripts, two kinds of forward primers were designed, one is close to the TSS site (S0), and another one is located on the upstream of TSS site (S-57) (Figure S7). As a result, the cDNAs could be amplified by S0/A + 784, and no products were detected by using S-57/A + 784. The plasmids expressed the RNAs with right size as proposed, it is receivable that the plasmids transcribed the SANTI1s start from the putative TSS site of the vector. Loops A and B highlighted similarities in the secondary structure between SANTI-S1 and the 3' terminal of wild-type SANTI.

The three types of SANTI were transfected in RCC cells and the total RNAs and proteins were harvested after 48 h. SANTI-S1 showed the similar inductive effect as wild type SANTI. As shown in Figure 3(b,c), the expression of the *SLC47A2* coding region was significantly increased by overexpressing SANTI or SANTI-S1, whereas

SANTI-S2 could not induce gene expression, irrespective of its sequence similarity with SANTI-S1. This suggested that a perfect secondary structure is the primary requirement for SANTI function, and that SANTI might act as a molecular scaffold for constructing RNP complexes.

### SANTI induced off-target binding of E2F1/HDAC1 to the coding gene promoter

As described earlier, SANTI might be involved in gene regulation *via* formation of functional lncRNA-protein complexes. To determine the members of this complex, computational analysis was performed to investigate lncRNA-protein interactions. According to the results of the catRAPID omic analysis, the SFPQ protein was forecast to be a strong partner of SANTI and SANTI-S1 (Table S3). However, SFPQ also exhibited weak interaction with SANTI-S2, irrespective of its differential secondary structure. We further analysed the binding site of SFPQ in the coding gene's promoter (from -5000 to +300) using the LASAGNA-Search 2.0 software and observed one SFPQ binding site in section 1 (Figure 3(d), in P1 promoter, -4450).

We confirmed a direct interaction between SANTI1s and SFPQ using cross-linking and immunoprecipitation (CLIP) (Figure 3(e)). In brief, we transfected pcDNA3.1 (NC), SANTI1, SANTI-S1, or SANTI-S2 into 769-P cells and purified the SANTI1-protein complex after 48 h using two biotin-labelled antisense oligonucleotides (ASOs). The presence of SFPQ in the purified samples was detected using western blot analysis. As shown in Figure 3(e), SFPQ was detected in SANTI or SANTI-S1 expressing 769-P using ASO-1 and ASO-2. In the blank plasmid group (NC), the constitutive expression of SANTI

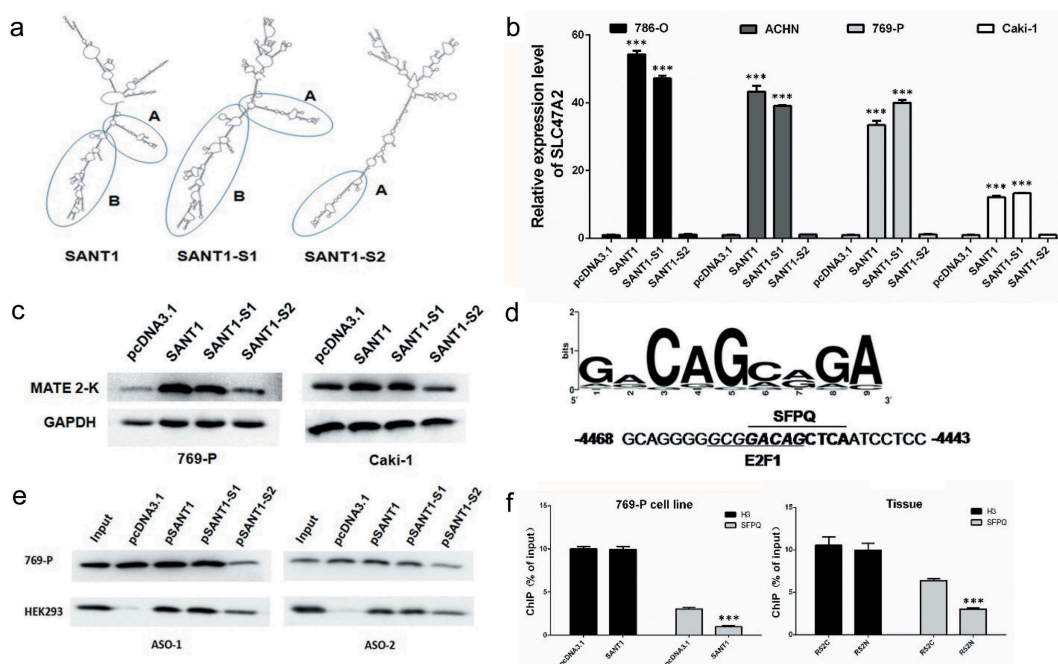


**Figure 3.** Secondary structure and functions of SANTI1, SANTI1-S1, and SANTI1-S2. (a) The secondary structure of the three SANTI1s. (b, c) The perfect secondary structure is the primary requirement for SANTI1-mediated promotion of *SLC47A2* expression. (d) The binding site of SFPQ in the coding gene promoter. (e) Direct interaction between SANTI1s and SFPQ. (f) Overexpression of SANTI1 significantly inhibited the binding of SFPQ to the coding gene promoter in 769-P cells and adjacent tissue.

was recognized using ASOs, and the presence of SFPQ was also detected. In contrast, in SANTI1-S2-transfected 769-P cells, we observed weak exposure of SFPQ. These results suggested that SANTI1-S2 might exhibit a weaker binding activity because of its different structures, which is in agreement with the results of the catRAPID omics report (Table S3). Another possibility was that the defective structure of SANTI1-S2 completely impaired the binding of SFPQ; however, the ASOs purified the SFPQ interacted with the constitutively expressed SANTI1, and this kind of interaction between ASOs and SANTI1 could be competitively inhibited by high levels of SANTI1-S2.

To further understand whether SANTI1-S2 retained the SFPQ binding ability, we investigated CLIP samples from HEK-293 cells (Figure 3(e)). Constitutive SANTI1 expression was low in HEK-293 cells, and no SFPQ was detected in the NC group. SFPQ was detected in the samples purified from three SANTI1-expressing cells, and fully functional SANTI1s (SANTI1 and SANTI1-S1) exhibited stronger binding abilities than the activation-deficient one (SANTI1-S2).

Thus, we concluded that SFPQ is one of the members of the SANTI1-associated regulatory complex. SANTI1-S2 exhibited weak binding with SFPQ but could not activate gene expression. Considering the significant change in SANTI1-S2 secondary structure, we suggested that perfect secondary structure of SANTI1 is necessary for forming the intact complex, and that the missing structure in SANTI1-S2 might be involved in interacting with other proteins of the regulatory complex.

To confirm the interaction between SANTI1 and SFPQ, we determined the binding rates of SFPQ in the coding gene's promoter (Figure 3(f)). SANTI1 and the blank plasmid were transfected into 769-P cells, and as described previously,

SANTI1 strongly upregulated the expression of the coding gene (Figure 2(f)). In contrast, high SANTI1 expression significantly suppressed the binding of SFPQ to the coding gene's promoter. In addition, the binding level of SFPQ was significantly higher in RCC tissue (R52C) than in paired adjacent tissue (R52N). Owing to higher SANTI1 level in adjacent tissues (Figure 1(g)), we suggested that a high level of SANTI1 inhibited the binding of SFPQ on the coding gene promoter. It appears that SFPQ binding to the promoter restrained the transcriptional activity by forming a gene repressor complex.

As reported previously, SFPQ frequently acts as a molecular scaffold at target promoters and participates in epigenetic silencing *via* formation of a corepressor complex by recruiting SIN3A and histone deacetylases (HDAC1 or HDAC3) [17, 18]. Previously, we have shown that E2F1 might be involved in restricting histone acetylation (H3K27ac) of the *SLC47A2* promoter by recruiting HDAC10 (5). E2F1/HDAC1 and E2F1/HDAC3 are also well known for inhibiting gene expression by suppressing the H3K27ac modification at gene promoters [5]. Considering the common function of SFPQ and E2F1 in recruiting HDACs, we predicted that the SFPQ/E2F1/HDAC1 complex is instrumental in repressing *SLC47A2*. Furthermore, the SFPQ binding site on the *SLC47A2* promoter is in proximity to an E2F1 binding site, which indicates that these proteins might interact physically (Figure 3(d)).

The formation of the SFPQ/E2F1/HDAC1 complex was confirmed in 769-P using the co-immunoprecipitation (co-IP) assay. We selected SFPQ, E2F1, or HDAC1 as the target protein, and precipitated the entire complex from the total cell lysate using anti-SFPQ, anti-E2F1, or anti-HDAC1 antibodies, respectively. As shown in Figure 4(a), we successfully determined the existence of

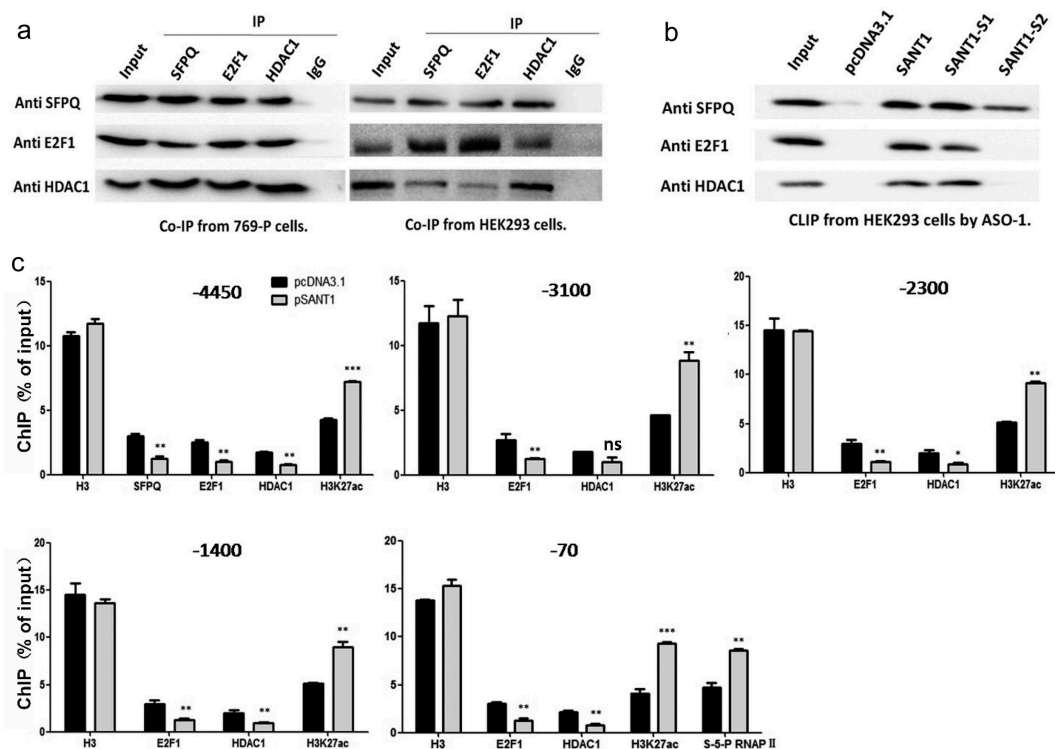


**Figure 4.** SANT1 altered the binding of SFPQ/E2F1/HDAC1 to the coding gene promoter. (a) Formation of the transcription suppressor SFPQ/E2F1/HDAC1 complex. (b) The perfect secondary structure of SANT1 is necessary for the formation of a functional RNP complex. (c) High expression of SANT1 promotes H3K27ac modification and S-5-P RNAPII binding to the *SLC47A2* promoter by inducing off-target binding of E2F1/HDAC1 to the coding gene promoter.

SFPQ, E2F1, and HDAC1 in each co-IP sample, which strongly suggested the existence of the SFPQ/E2F1/HDAC1 complex. To further verify the relationship between SANT1 and the SFPQ/E2F1/HDAC1 complex, we performed the co-IP assay in HEK293 cells, which expresses extremely low levels of SANT1, and confirmed the formation of the SFPQ/E2F1/HDAC1 complex in the absence of SANT1. Therefore, we proposed two potential mechanisms: 1) SANT1 is involved in target binding of the SFPQ/E2F1/HDAC1 complex at the *SLC47A2* promoter but is not necessary for its formation; 2) SANT1 participates in the formation of the *SLC47A2*-regulatory complex, but does not affect the formation of other similar regulatory complexes.

To confirm the role of SANT1 in the formation of the SFPQ/E2F1/HDAC1 complex, we transfected the blank vector, SANT1, SANT1-S1, or SANT1-S2 into HEK293 cells and then purified RNA-binding proteins *via* CLIP using ASO-1 as the probe. As shown in Figure 4(a), the members of the SFPQ/E2F1/HDAC1 complex were detected in each precipitated sample. All members were detected in cells expressing SANT1 and SANT1-S1, but only SFPQ was detected in cells expressing SANT1-S2 (Figure 4(b)). Considering the extreme differences in secondary structure between SANT1/SANT1-S1 and SANT1-S2, we concluded that the perfect secondary structure of SANT1 is necessary for forming a functional RNP complex.

To further understand the function of SANT1 in regulating the binding of the SFPQ/E2F1/HDAC1 complex to the promoter, we overexpressed SANT1 in 769-P cells and detected the binding rate of the SFPQ/E2F1/HDAC1 complex to the entire *SLC47A2* promoter (Figure 4(c)). According to the computational analysis of binding of transcription factors, the coding gene's promoter contained only one SFPQ (-4450) binding site, which was in

proximity to an E2F1 binding site (Figure 3(d)). We also detected abundant E2F1 binding sites from -4000 to +1 in the coding gene's promoter. Therefore, the other four E2F1 binding sites (-3100, -2300, -1400, and -70) were also selected for determining the E2F1/HDAC1 binding rate after overexpressing SANT1 in 769-P cells.

As shown in Figure 4(c), overexpression of SANT1 reduced the binding rate of SFPQ/E2F1/HDAC1 to the SFPQ (also E2F1) binding site in the promoter region. On the contrary, the level of H3K27ac, which is regulated by HDAC1, increased significantly. In addition, the extent of E2F1/HDAC1 binding was also significantly reduced at the other E2F1 promoter binding sites. These results showed that the level of the H3K27ac modification increased over the entire *SLC47A2* promoter and that the binding of S-5-P RNAPII was strongly upregulated in the region proximal to the TSS. This suggested that SANT1 overexpression resulted in higher level of H3K27ac modification and S-5-P RNAPII binding in the *SLC47A2* promoter by inducing off-target binding of E2F1/HDAC1.

## Discussion

*SLC47A2* was identified as a promising diagnostic biomarker and is considered to be tightly associated with risk of developing RCC as its transcription is significantly repressed in all patients tested [5]. Furthermore, univariate analyses indicated that *SLC47A2* expression is a prognostic risk factor for patients with RCC, and lower level of *SLC47A2* might act as a negative prognostic marker (Figure 1(c)). *SLC47A2* expression is strongly suppressed in RCC (Figure 1(a,b)), which might significantly change the function of kidney cells in excreting anti-cancer drugs and endogenous

substances [5]. However, evidence regarding the role of *SLC47A2* in RCC aetiology or progression is absent.

With the development of large-scale sequencing technology, the aberrant transcriptional profiles and transcription regulatory mechanisms in kidney cancer were investigated, and many ncRNAs were found to be involved in the progression of kidney cancer [19,20]. The abnormal expression of ncRNAs plays important roles in tumour genesis, growth, or metastasis through their interactions with other cellular macromolecules [21]. Accumulating evidence suggests that lncRNAs are important regulators of almost all gene expression networks and are involved in regulatory processes, ranging from epigenetic, transcriptional, and post-transcriptional processes [22].

Depending on their functional models, lncRNAs can regulate adjacent or own loci *via cis* regulation, or regulate distal genes *via trans* regulation [23]. In this study, we focused on detecting the *cis* regulatory model of *SLC47A2*. Initiation and elongation of most lncRNAs require the same transcriptional machinery as other mRNAs, and lncRNAs are regulated by RNAPII occupancy, transcription factor binding, and histone modifications [23]. We obtained the full-length sequence of lncRNA *SANT1* by evaluating the binding rate of S-5-P RNAPII at the potential transcriptional regions in the *SLC47A2* locus, and finally confirmed the *cis* regulatory model of *SANT1* in four RCC cell lines.

Many lncRNAs display *cis* regulatory functions by altering transcription factor binding to gene promoter regions [24]. However, recent findings showed that certain functional micropeptides can be encoded by lncRNAs [15,16]. It appears that lncRNAs act as gene regulators by forming RNP complexes or translating functional micropeptides. To further understand the regulatory mechanism of *SANT1*, we analysed its secondary structure and constructed two *SANT1* mutants (Figure 3(a)). Figure 3(b,c) show that *SANT1* does not translate potential micropeptides but acts as a modular scaffold in activating the performance of the *SLC47A2* coding gene's promoter; additionally, *SANT1* must have a perfect secondary structure for forming a regulatory RNP complex (Figures 3,

4). Furthermore, lncRNAs act as miRNA sponge, thereby regulating miRNA expression, which in turn suppresses the targeted binding between specific genes and miRNAs [25]. It is also possible that *SANT1* regulates the expression of *SLC47A2* through lncRNA–mRNA/miRNA interaction in RCC, which will be extensively studied in future.

The SFPQ protein was forecast to be a strong partner of *SANT1* and *SANT1*-S1 (Table S3), and we confirmed the direct binding between *SANT1*/*SANT1*-S1 and SFPQ using the CLIP assay. The binding rate of SFPQ to the *SLC47A2* promoter was significantly suppressed by high *SANT1* level (Figure 3(f)), which is indicative of the inhibitory ability of the SFPQ-associated functional complex. SFPQ/HDACs [17,18] and E2F1/HDACs [5] are well-known to repress gene expression by decreasing H3K27ac modification in the gene promoter. Considering that HDAC1 is the common member in SFPQ/HDAC and E2F1/HDAC complexes, we predicted that the SFPQ/E2F1/HDAC1 complex was a transcriptional repressor of *SLC47A2*. The existence of the SFPQ/E2F1/HDAC1 complex was verified using co-IP, and *SANT1* was involved in relocating the regulatory repressor from the promoter region. However, in tumour tissues, lower expression of *SANT1* and higher expression of E2F1 [5] resulted in significantly higher binding of E2F1/HDAC1 to the *SLC47A2* promoter, which repressed MATE 2-K by reducing H3K27ac modification and S-5-P RNAPII binding.

In this study, we observed that repression of *SLC47A2*, which was identified as a promising diagnostic biomarker, correlated positively with overall survival in 818 patients with RCC cancer (Figure 1(c)). While investigating the molecular mechanism underlying *SLC47A2* repression, we identified a novel human lncRNA, *SANT1*, which is transcribed from the *SLC47A2* locus. We identified a new mechanism of *SANT1*-mediated *SLC47A2* regulation, which involved the relocation of an inhibitory SFPQ/E2F1/HDAC1 complex from the promoter and increase in H3K27ac modification and S-5-P RNAPII binding. In RCC tissue, low *SANT1* expression increased E2F1/HDAC1 binding to the entire coding gene promoter, which induced a significantly lower level of histone H3K27ac modification (Figure 5). The *SANT1*-

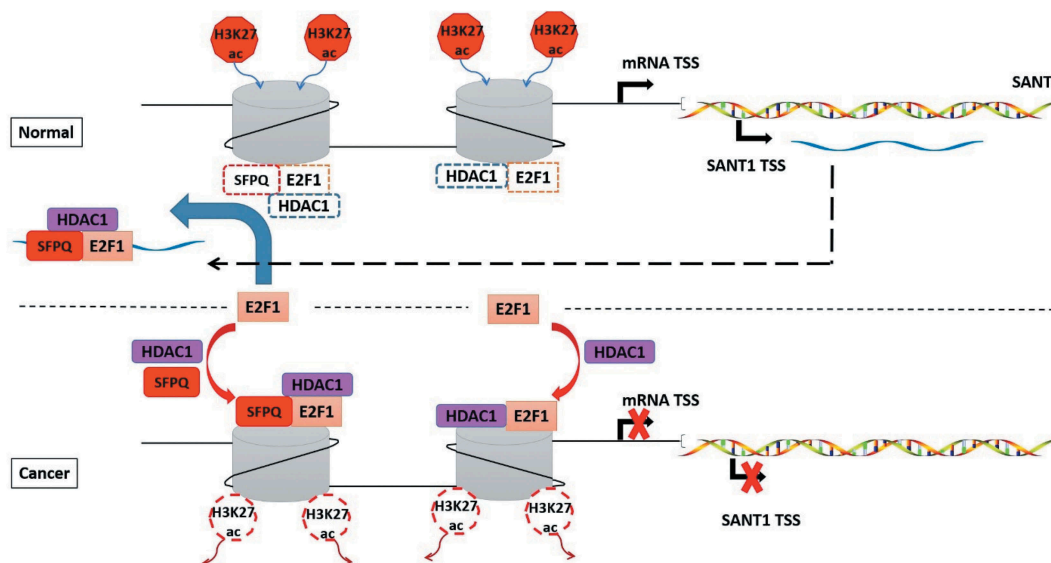


Figure 5. *SANT1* induced off-target binding of E2F1/HDAC1 to the entire coding gene promoter.

*SLC47A2* regulatory network promoted abnormal gene expression in RCC. Considering the tight correlation between *SANT1* and *SLC47A2* expression, *SANT1* expression level, as well as *SLC47A2* expression, can be used as a prognostic marker for RCC. However, the reason behind the extremely low *SANT1* level is still unclear, and the mechanism underlying the association of *SLC47A2* repression with poor prognosis in patients with renal cancer requires further investigation.

## Materials and methods

### Tissues and cell culture

The paired RCC samples were provided by the Specimen Bank of Zhejiang Cancer Hospital (Hangzhou) and were approved for use by the Zhejiang Cancer Hospital Ethics Committee ([2014]-08-76). Patients' clinical information is shown in Supplementary Table S1.

HEK293 and human RCC cell lines 786-O, 769-P, ACHN, and Caki-1 were purchased from the Chinese Academy of Science Committee on type culture collection cell libraries. HEK293 was cultured in Dulbecco's modified Eagle's medium (DMEM), 786-O and 769-P were cultured in Roswell Park Memorial Institute (RPMI) 1640 medium, ACHN was cultured in minimal essential medium (MEM), and Caki-1 was cultured in McCoy's 5 A medium. All media contained 10% fetal bovine serum, 100 U/mL penicillin, and 100 mg/mL streptomycin.

### Bioinformatic analysis

Potential promoter analysis of the *SLC47A2* locus was performed using the UCSC genome browser (GRCh37/hg19). *SANT1* secondary structure prediction was performed on M-Fold. *SANT1*-protein interaction was predicted using catRAPID. SFPQ and E2F1 binding sites analysis were performed using LASAGNA-Search 2.0 and PROMO, respectively. In the current study, the prognostic values of *SLC47A2* in RCC were analysed using KM plotter, which updated gene expression data and survival information from 818 patients with renal cancer.

### Chromatin immunoprecipitation assay (ChIP)

ChIP was performed per the protocol of the ChIP assay kit (Beyotime, P2078). In briefly, RCC samples were fully shredded with scissors and ground with a homogenizer, and then were rotational cross-linked with 1% formaldehyde for 30 min, cells were cross-linked with 1% formaldehyde for 10 min at 37°C. Then the samples were neutralized with glycine for 5 min at room temperature, all samples were washed by cold PBS, then collected and stored on ice. Next, the samples were lysed with SDS lysis buffer, and DNA was shredded to fragments of 200–1000 bp by sonication. An equal amount of chromatin was immunoprecipitated at 4°C overnight with 1.5 µg of the following antibodies: anti-H3 (Abcam, ab1791, 1mg/ml), anti-S-5-P RNAPII (Abcam, ab5095, 1mg/ml), anti-SFPQ (GeneTex, GTX114209, 1.36mg/ml), anti-E2F1 (GeneTex, GTX101235, 1mg/ml), anti-HDAC1 (GeneTex, GTX100513, 1mg/ml), and anti-H3K27ac (Abcam, ab4729, 1mg/ml).

Antibodies were added to each aliquot of pre-cleared chromatin and incubated overnight. Protein A + G-agarose beads were added and incubated for 2 h at 4°C. After reversing the cross-links, the immunoprecipitated DNA was purified and subjected to qPCR analysis, and the primers used are listed in Supplementary Table S2.

### RACE of *SANT1*

Total RNA (2 µg) from adjacent (R39N) tissue was reverse transcribed using the primer 3-AD, which contains a lock-docking oligo (dT). The three rounds of 3' RACE PCR were performed using 3RACE-S1/NUP, 3RACE-S2/NUP, and 3RACE-S3/NUP.

5' RACE amplification was performed using the ribonucleotide tailing method. Total RNA (4 µg) was reverse transcribed using the primer 5RACE-A1. The cDNA mixture was incubated with RNase H for 1 h at 37°C, and then the cDNA was processed to generate a ribo-tail using terminal deoxynucleotidyl transferase (TdT) (Takara, 2230A) and rCTP. The first round of PCR was performed using 5-AD/5RACE-A2, and the following amplifications were performed using NUP/5RACE-A3, NUP/5RACE-A4, and NUP/5RACE-A5. All the primers are listed in Supplementary Table S2.

### Plasmid construction

Full-length *SLC47A2* mRNA, *SANT1*, and *SANT1* mutants (*SANT1*-S1 and *SANT1*-S2) were cloned into the pcDNA3.1(+) vector. The *SLC47A2* mRNA was amplified using mRNA-S/mRNA-A. Full-length *SANT1* and *SANT1*-S1 were amplified using *SANT1*-S/*SANT1*-A and *SANT1*-S1/*SANT1*-A1, respectively. *SANT1*-S2 was amplified from *SANT1*-S1 using *SANT1*-S2/*SANT1*-A2. The *SLC47A2* mRNA and *SANT1*-S1 were sub-cloned into the *EcoR* V restriction enzyme site. *SANT1* was sub-cloned between *Sac* I/*Xho* I restriction enzyme sites, and *SANT1*-S2 was sub-cloned into *Sac* I/*Xba* I sites. The differences between the three forms of *SANT1* are shown in Supplementary Figure S1 and primers are shown in Supplementary Table S2.

To confirm the transcriptional start site of the rescued *SANT1*s transcripts, total RNAs from the plasmid-rescued cells were extracted as described before. The RNAs were treated by DNase I and reverse transcribed using the primer A923. The PCR detections were carried out using S0/A784 or S-57/A784. The location of primers is shown in Supplementary Figure S6, and the sequences could be found in Supplementary Table S2.

### Real-time PCR

Total RNA was extracted using the total RNA mini-prep kit (Tiangen) and then reverse transcribed into cDNA with PrimeScript RT master mix (Takara). Real-time PCR was performed using the SYBR Premix EX Taq (Takara); the reaction system included 1 µL cDNA, 1 µL primer, 0.2 µL ROX dye, 4.8 µL SYBR® Premix Ex Taq™, and 3 µL double distilled H<sub>2</sub>O. mRNA expression level was normalized to glyceraldehyde-3-phosphate dehydrogenase (GAPDH) expression. The primers used are listed in Supplementary Table S2.



### Western blot analysis

Cells were cultured in six-well plate, washed with phosphate buffered saline (PBS) after maturation, harvested with 0.25% trypsin, and then lysed using radioimmunoprecipitation assay (RIPA) (Beyotime, P0013B) supplemented with phenylmethylsulfonyl fluoride. The concentrations of the protein samples were quantified using the bicinchoninic acid (BCA) protein assay kit (Beyotime). Equal amounts of protein extracts were separated using 10% sodium dodecyl sulfate-polyacrylamide gel electrophoresis (SDS-PAGE) and then transferred to polyvinylidene fluoride (PVDF) membranes. The PVDF membranes were blocked for 2 h in 5% nonfat milk and incubated overnight with primary antibodies at 4°C, followed by incubation with secondary antibodies for 2 h at room temperature. Finally, the PVDF membranes were exposed to colouration using G-box. MATE 2-K antibody (Sigma, HPA062112, 1:200 dilution) was used in western blot analysis.

### Co-IP

Cells were cultured in a 10-cm cell culture dish and washed with PBS after maturation. The cells were digested with 0.25% trypsin and collected into 1.5 mL tubes. The cells were washed once with precooled PBS. Whole cell lysates were prepared using Pierce™ IP lysis buffer (Thermo, 87787) supplemented with protease inhibitors. Lysates were incubated with 2 µg of antibodies and 30 µl of protein A + G agarose (Beyotime, P2012). The complexes were collected by centrifugation. Target proteins were detected using western blot analysis. Antibodies used for co-IP included anti-SFPQ (GeneTex, GTX114209, 1.36mg/ml), anti-E2F1 (GeneTex, GTX101235, 1mg/ml), anti-HDAC1 (GeneTex, GTX100513, 1mg/ml), and anti-IgG (Santa Cruz, sc-2027, 1mg/ml).

### CLIP

Cells were cultured in a 10-cm cell culture dish. The cells were exposed to UV light to crosslinking the protein-RNA complexes in vivo. Cells were harvested by trypsinization and washed three times with pre-cooled PBS. PBS was removed and 2 ml of lysis buffer (Thermo Fisher, 87788) supplemented with protease, RNase, and DNase inhibitors were added to the pellet to lyse the cells. The lysate was centrifuged at 12,000 g for 10 min at 4°C, and the supernatant collected for RNA isolation. Protein concentration of eluate was determined with the BCA method. ~35 µg protein was transferred to a 1.5 ml tube, then incubated with 200 pmol of antisense oligonucleotides (ASOs), mixed and incubated at 70°C for 5 min. ASOs used in CLIP are listed in Supplementary Table S2. Blocked streptavidin agnetic beads were added, and the mixture was incubated for 30 min at room temperature with constant shaking. The beads were retrieved using a magnet and the supernatant was collected for reference. The beads were then washed three times with 750 µl B&W buffer (10 mM Tris-HCl, pH 7.5, 150 mM NaCl, 0.5 mM EDTA, pH 8.0) at 55°C. Finally, 50 µl of B&W buffer was added and the sample split: 20 µl for RNA and 30 µl for protein analysis. Removed the B&W buffer and the beads were resuspended by 20 µl of Tris-HCl (10 mM, pH 7.5) and then incubated at 90°C for 10 min until the RNA released from beads. For protein analysis, the beads were

resuspended in 20 µl of Laemmli buffer and denatured at 100°C for 5 min.

### Statistical analysis

Results are presented as mean ± standard deviations (SD). Statistical comparisons were made using the Mann–Whitney test in GraphPad Prism 5, and differences between groups were considered significant if the P value was <0.05.

### Acknowledgments

We thank Ms. Haihong Hu for managing the instruments and helping us perform the experiments.

### Complying with ethics of experimentation

The procedures used in this study were approved by the Zhejiang Cancer Hospital Ethics Committee ([2014]-08-76).

### Data deposition

The nucleotide sequence of SANT1 has been submitted to the GenBank with the accession number MH971975.

### Data availability statement

The data that support the finding of this study are available from the corresponding author (Su Zeng and Lushan Yu), upon reasonable request.

### Disclosure statement

No potential conflict of interest was reported by the authors.

### Funding

This work was supported by the [National Natural Science Foundation of China] under Grant [number 81773817] and [Key Technologies R&D Program of China] under Grant [number 2017YFC0908600].

### References

- [1] Ljungberg B, Bensalah K, Canfield S, et al. EAU guidelines on renal cell carcinoma: 2014 update. *Eur Urol*. 2015;67:913–924.
- [2] Ferlay J, Soerjomataram I, Dikshit R, et al. Cancer incidence and mortality worldwide: sources, methods and major patterns in GLOBOCAN 2012. *Int J Cancer*. 2014;136:E359–E386.
- [3] Liu Y, Zheng X, Yu Q, et al. Epigenetic activation of the drug transporter OCT2 sensitizes renal cell carcinoma to oxaliplatin. *Sci Transl Med*. 2016;8(348):348ra97.
- [4] Zheng X, Liu Y, Yu Q, et al. Response to Comment on “Epigenetic activation of the drug transporter OCT2 sensitizes renal cell carcinoma to oxaliplatin”. *Sci Transl Med*. 2017;9(391):eaam6298.
- [5] Yu Q, Liu Y, Zheng X, et al. Histone H3 lysine 4 trimethylation, lysine 27 trimethylation, and lysine 27 acetylation contribute to the transcriptional repression of solute carrier family 47 member 2 in renal cell carcinoma. *Drug Metab Dispos*. 2017;45:109.
- [6] Omote H, Hiasa M, Matsumoto T, et al. The MATE proteins as fundamental transporters of metabolic and xenobiotic organic cations. *Trends Pharmacol Sci*. 2006;27:587–593.
- [7] Damme K, Nies AT, Schaeffeler E, et al. Mammalian MATE (SLC47A) transport proteins: impact on efflux of endogenous substrates and xenobiotics. *Drug Metab Rev*. 2011;43:499–523.

- [8] Staud F, Cervený L, Ahmadimoghaddam D, et al. Multidrug and toxin extrusion proteins (MATE/SLC47); role in pharmacokinetics. *Int J Biochem Cell Biol.* **2013**;45:2007–2011.
- [9] Kapranov P, Cheng J, Dike S, et al. RNA maps reveal new RNA classes and a possible function for pervasive transcription. *Science.* **2007**;316:1484.
- [10] Fok ET, Scholefield J, Fanucchi S, et al. The emerging molecular biology toolbox for the study of long noncoding RNA biology. *Epigenomics.* **2017**;9:1317–1327.
- [11] Quinn JJ, Chang HY. Unique features of long non-coding RNA biogenesis and function. *Nat Rev Genet.* **2015**;17:47.
- [12] Jain S, Thakkar N, Chhatai J, et al. Long non-coding RNA: functional agent for disease traits. *RNA Biol.* **2017**;14(5):522–535.
- [13] Zhu L, Xu PC. Downregulated lncRNA-ANCR promotes osteoblast differentiation by targeting EZH2 and regulating Runx2 expression. *Biochem Biophys Res Commun.* **2013**;432:612–617.
- [14] Hafner M, Landthaler M, Burger L, et al. Transcriptome-wide identification of RNA-binding protein and microRNA target sites by PAR-CLIP. *Cell.* **2010**;141:129–141.
- [15] Anderson Douglas M, Anderson Kelly M, Chang C-L, et al. A micropeptide encoded by a putative long noncoding RNA regulates muscle performance. *Cell.* **2015**;160:595–606.
- [16] Bazzini AA, Johnstone TG, Christiano R, et al. Identification of small ORFs in vertebrates using ribosome footprinting and evolutionary conservation. *Embo J.* **2014**;33(9):981–993.
- [17] Snijders AP, Hautbergue GM, Bloom A, et al. Arginine methylation and citrullination of splicing factor proline- and glutamine-rich (SFPQ/PSF) regulates its association with mRNA. *Rna.* **2015**;21:347–359.
- [18] Knott GJ, Bond CS, Fox AH. The DBHS proteins SFPQ, NONO and PSPC1: a multipurpose molecular scaffold. *Nucleic Acids Res.* **2016**;44:3989–4004.
- [19] Yu G, Yao W, Wang J, et al. LncRNAs expression signatures of renal clear cell carcinoma revealed by microarray. *PLOS ONE.* **2012**;7:e42377.
- [20] Blondeau JJC, Deng M, Syring I, et al. Identification of novel long non-coding RNAs in clear cell renal cell carcinoma. *Clin Epigenetics.* **2015**;7:10.
- [21] Schmitt AM, Chang HY. Long noncoding RNAs in cancer pathways. *Cancer Cell.* **2016**;29:452–463.
- [22] Zhang X, Hamblin MH, Yin K-J. The long noncoding RNA Malat1: its physiological and pathophysiological functions. *RNA Biol.* **2017**;14(12):1705–1714.
- [23] Mercer TR, Mattick JS. Structure and function of long noncoding RNAs in epigenetic regulation. *Nat Struct Mol Biol.* **2013**;20:300.
- [24] Zhang B, Arun G, Mao YS, et al. The lncRNA Malat1 is dispensable for mouse development but its transcription plays a cis-regulatory role in the adult. *Cell Rep.* **2012**;2(1):111–123.
- [25] Song X, Cao G, Jing L, et al. Analysing the relationship between lncRNA and protein-coding gene and the role of lncRNA as ceRNA in pulmonary fibrosis. *J Cell Mol Med.* **2014**;18:991–1003.